Lab 4

Navigation with IMU and Magnetometer

Data Collection and Initial Analysis

In this phase, we meticulously collected data using both GPS and IMU sensors. The IMU was securely mounted in the vehicle with the x-axis aligned to its forward direction, while the GPS sensor was fixed on the vehicle's roof. Both sensors were connected to our data logging system. After an initial 10-second delay, we initiated the vehicle's movement, following a planned course with 360-degree turns for compass calibration. The data collection was executed with precision, with the usage of the autonomous car 'NUANCE'.

Data Analysis and Yaw Angle/Velocity/Trajectory Estimation

Our data analysis primarily focused on estimating the vehicle's yaw angle, a crucial component of our navigation system. To accomplish this, we commenced with magnetometer calibration. This calibration involved correcting magnetometer readings for "hard-iron" and "soft-iron" effects, leveraging data collected during circular motion.

We visually documented the magnetometer data before and after correction, facilitating a before-and-after comparison. The yaw angle was estimated through two distinct methods: magnetometer-based and yaw rate sensor integration. The results from these methods were meticulously compared to assess their alignment and potential discrepancies.

A pivotal step in our analysis was the application of a complementary filter. This filter expertly combined magnetometer and yaw rate sensor measurements to enhance yaw angle estimation. The resulting complementary filter output provided a more robust and precise yaw angle estimation.

In parallel, we compared our results to the yaw angle computed by the IMU, adding a layer of validation to our analysis.

Our data collection, analysis, and estimation techniques set the stage for a deeper exploration of dead reckoning with IMU technology. The yaw angle estimation and velocity analysis are fundamental components in comprehending the vehicle's motion and navigation, forming the basis of our subsequent investigations.

Magnetometer Calibration

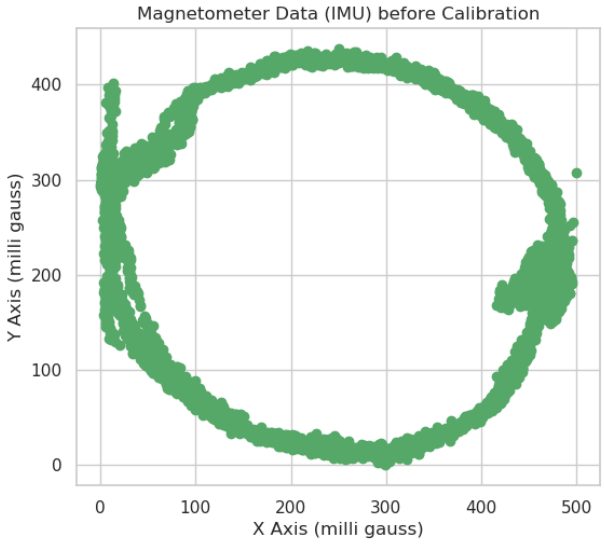

Hard iron errors in IMUs stem from constant offsets in magnetic field readings caused by nearby ferrous materials. Soft iron errors are the result of nonlinear distortions in the magnetic field due to the sensor's enclosure and materials. Calibration methods, including offset corrections for hard iron errors and ellipsoid fitting for soft iron errors, are used to eliminate these errors, enhancing the reliability of IMU measurements for applications like orientation estimation and navigation.

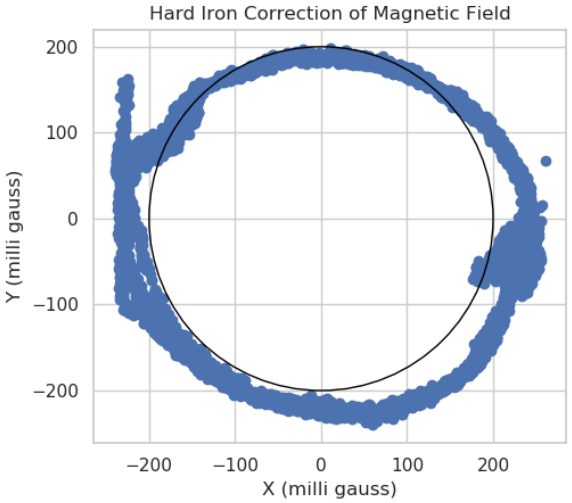

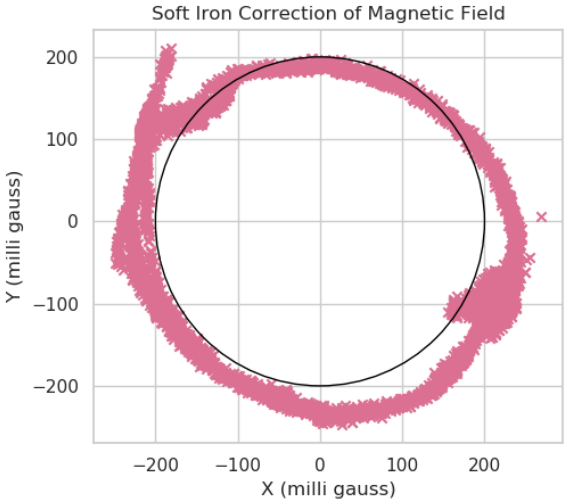

Adjusted Transformation Matrix based on data collected to eliminate soft-iron and hard-iron errors:

$$\begin{bmatrix} \cos(0.233) & -\sin(0.233) & 0 \\ \sin(0.233) & \cos(0.233) & 0 \\ 0 & 0 & 1 \end{bmatrix} \begin{bmatrix} Mx - & 239.27 \\ My- & 239.09 \end{bmatrix}$$

Yaw Estimation (Heading)

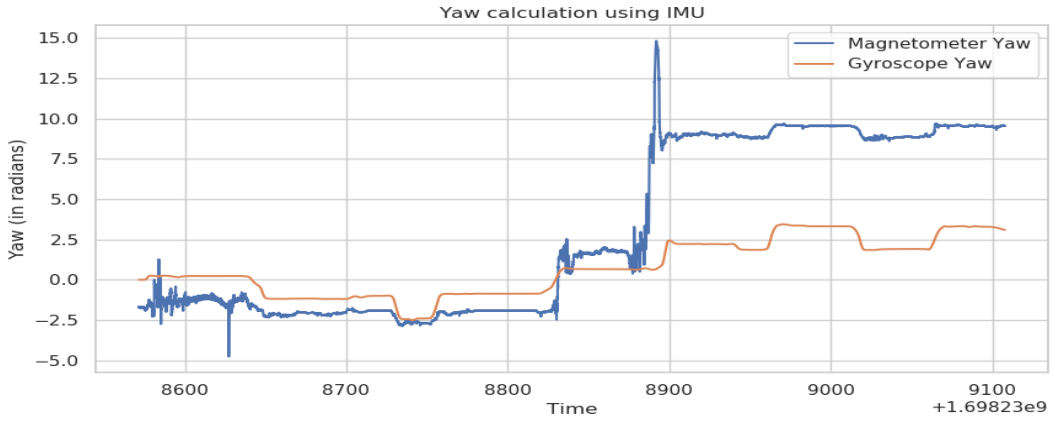

To determine the yaw angle, we employed a multifaceted approach, comparing results from different methods. Initially, we integrated the yaw rate sensor data to obtain the yaw angle. This integration process involved treating the time series as a function and utilizing the 'trapz' or 'cumtrapz' commands in Matlab. Simultaneously, we calculated the yaw angle using magnetometer readings, based on the arctan(-y/x), where 'y' and 'x' were the corrected Magnetic_Y and Magnetic_X values. The resulting corrected magnetic yaw was unwrapped to eliminate discontinuities.The resulting corrected magnetic yaw was unwrapped to eliminate discontinuities, and then passed through a low pass filter (LPF) with a passband frequency of 0.25

In parallel, we integrated the gyro_z data, which represented angular velocity in the z-axis. The integrated value was processed through a high pass filter (HPF) with a passband frequency set to 0.75 Hz. This yielded the HPF output. In the complementary filter approach, we combined the LPF and HPF outputs to enhance the estimation of the yaw angle. By summing the LPF and HPF values, we derived the complementary filter output, providing a more robust estimation. The graphs of the LPF, HPF, and complementary filter output were meticulously plotted and are presented in our report for comprehensive analysis.

Comparing these methods, we evaluated the yaw angle results and scrutinized any differences between the magnetometer-based estimate and the integrated yaw from the gyro.

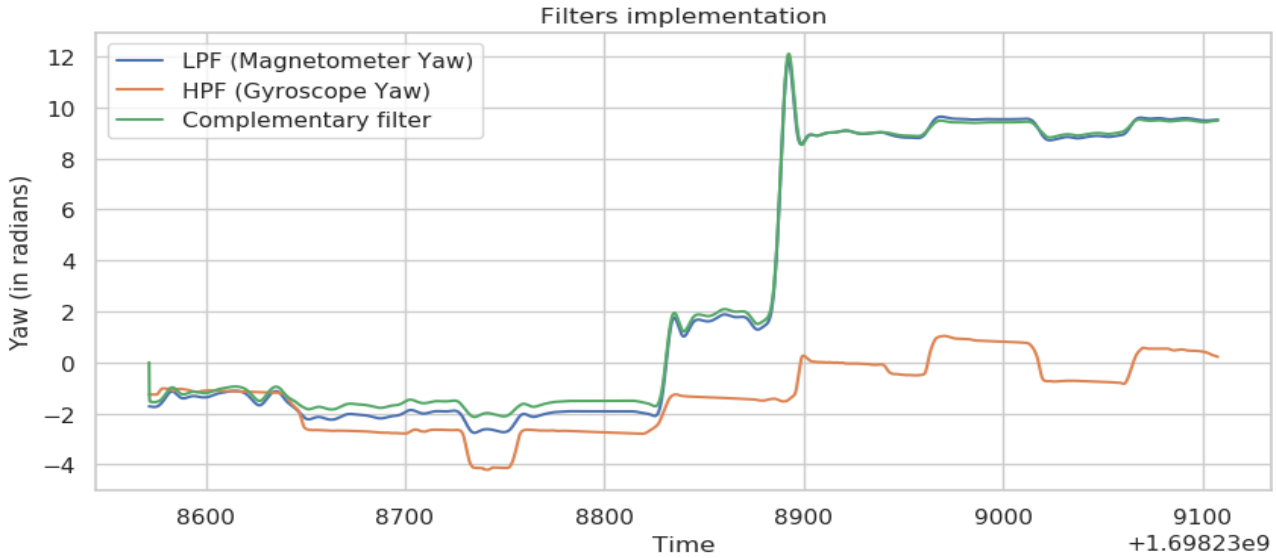

Velocity Estimation

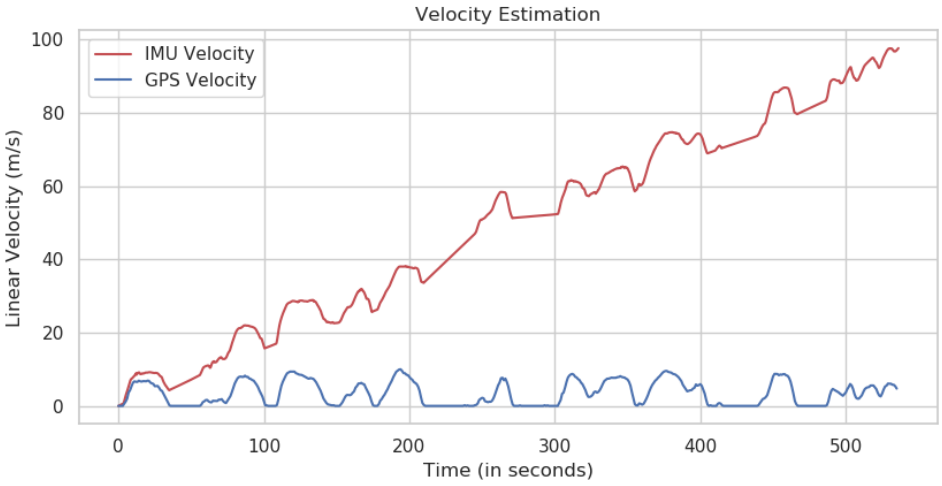

Before making adjustments, direct integration of IMU acceleration data resulted in linearly increasing velocity values, even during stationary periods. This increasing nature can be attributed to the bias being integrated overtime. To address this, a bias correction method was applied. This correction included identifying stationary segments using a line of best fitting method and subtracting the mean acceleration during these segments.

Post-adjustment, the IMU-derived velocity closely matches the GPS velocity, calculated using *V=S/T*. The primary adjustment was bias removal from the Linear Acceleration before integration to obtain Linear Velocity. One more discrepancy could be the presence of negative IMU-derived velocity, which may require further high-level filtering. Despite this, IMU velocity estimates hold potential for indoor navigation where GPS signals are limited.

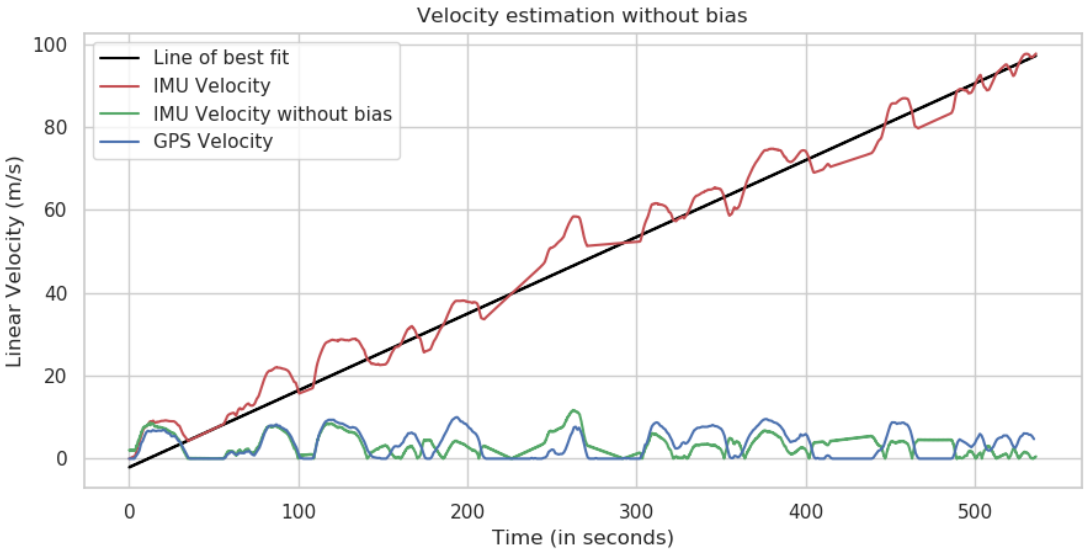

Dead Reckoning

Our IMU-based dead reckoning strategy began with data integration to estimate vehicle displacement. A two-dimensional motion model, considering vehicle position (X, Y, 0) and rotation rate (0, 0, ω), guided the process. After addressing lateral skidding and eliminating offsets, we refined forward acceleration representation for improved estimation. Integrating this adjusted acceleration yielded forward velocity, which we meticulously compared with GPS data, scrutinizing disparities and their causes.

To enhance precision, we employed magnetometer-derived heading data to transform velocity into a fixed (East, North) reference frame (ve, vn). Integrating this transformed velocity provided a precise vehicle trajectory (xe, xn). We meticulously aligned starting points and directions of GPS and IMU-derived trajectories to ensure a rigorous side-by-side assessment. Any applied scaling factors for comparability were considered.